Supporting Information

High-performance transition metal single-atom-anchored IrN_2 monolayer as an electrocatalyst for nitrate reduction to ammonia

Jing Xu[a], Guangkun Yan[a], Zeyue Peng[a], Tao Ding[a], Yizhu Wang[a], Yuqi Qiu[a], Wenxi Han[a], Jifa Fu[a], Guang Zhao[b], Hao Ren[a], Wei Xing[a], and Lianming Zhao[a,*]

[a] Shandong Key Laboratory of Intelligent Energy Materials, School of Materials Science and Engineering, China University of Petroleum (East China), Qingdao, Shandong 266580, China

[b] School of Petroleum Engineering, China University of Petroleum (East China), Qingdao, Shandong 266580, China

*Corresponding authors.

E-mail addresses: lmzhao@upc.edu.cn (L. Zhao).

Table of contents

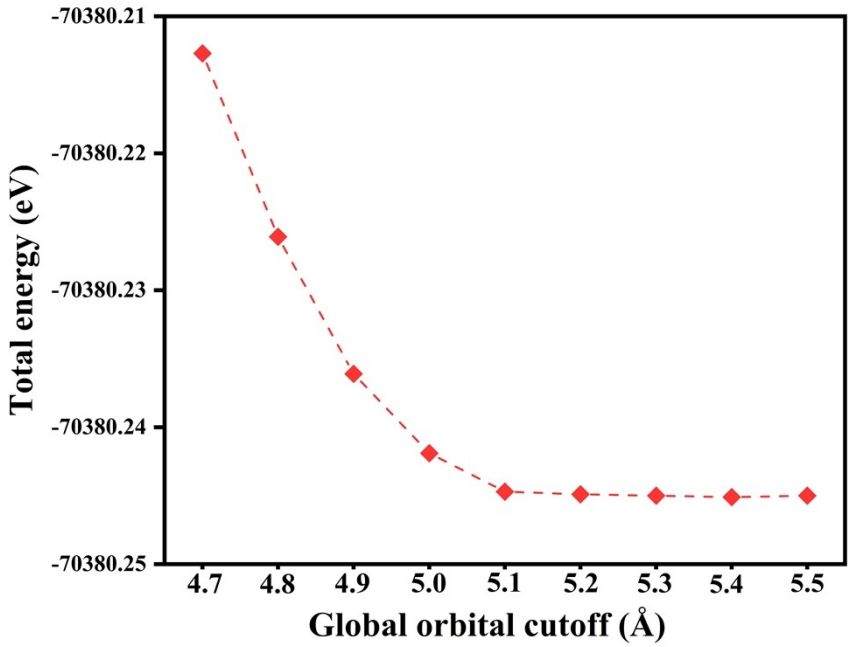

Fig. S1 Total energy of IrN_2 as a function of the global orbital cutoff.

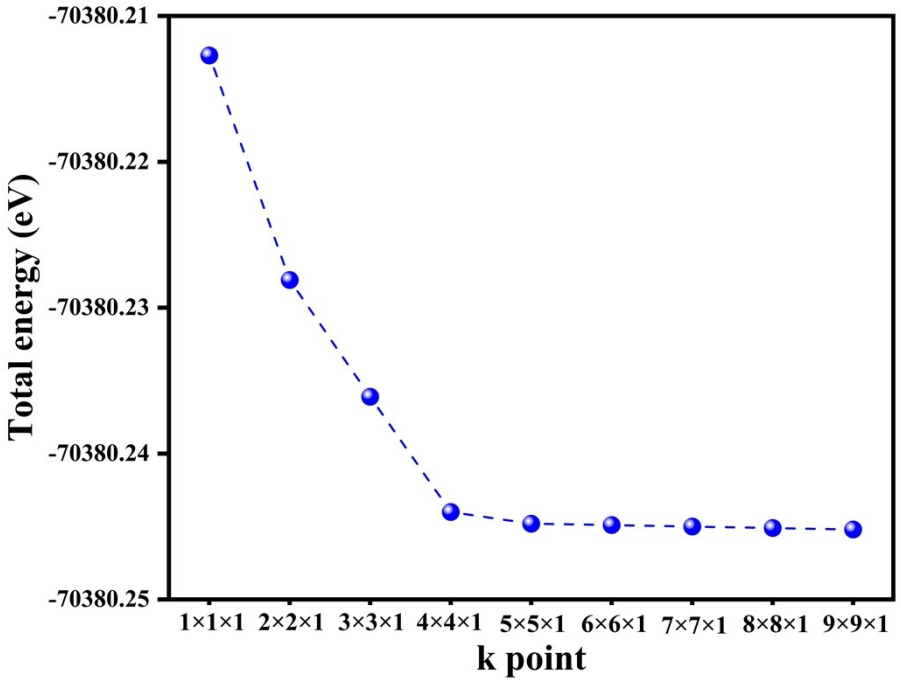

Fig. S2 Total energy of IrN_2 as a function of the k-point.

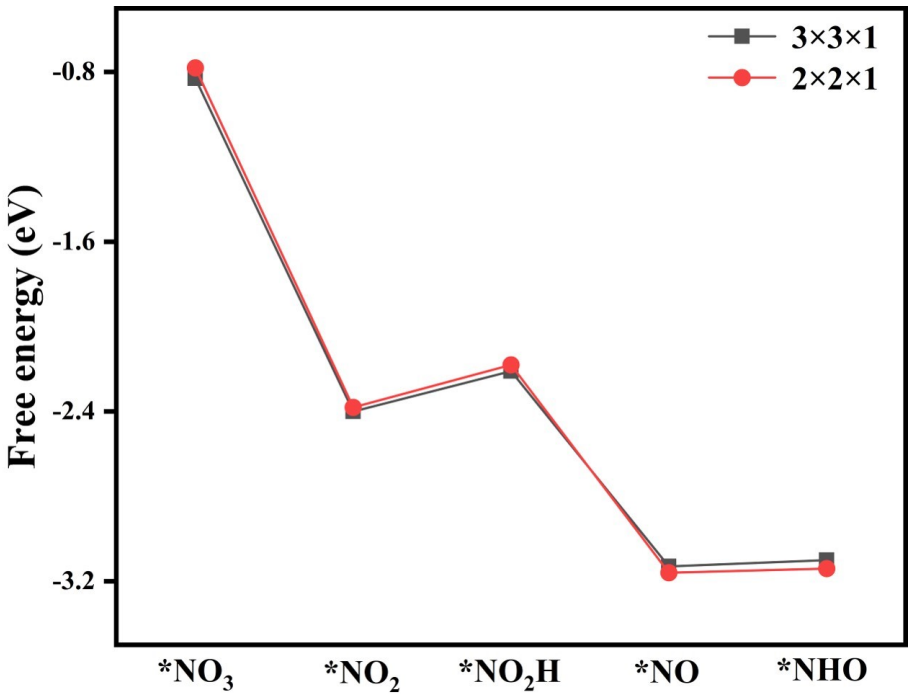

Fig. S3 Comparison of adsorption free energies of key intermediates on the 2×2×1 and 3×3×1 Ru-IrN_2 surfaces.

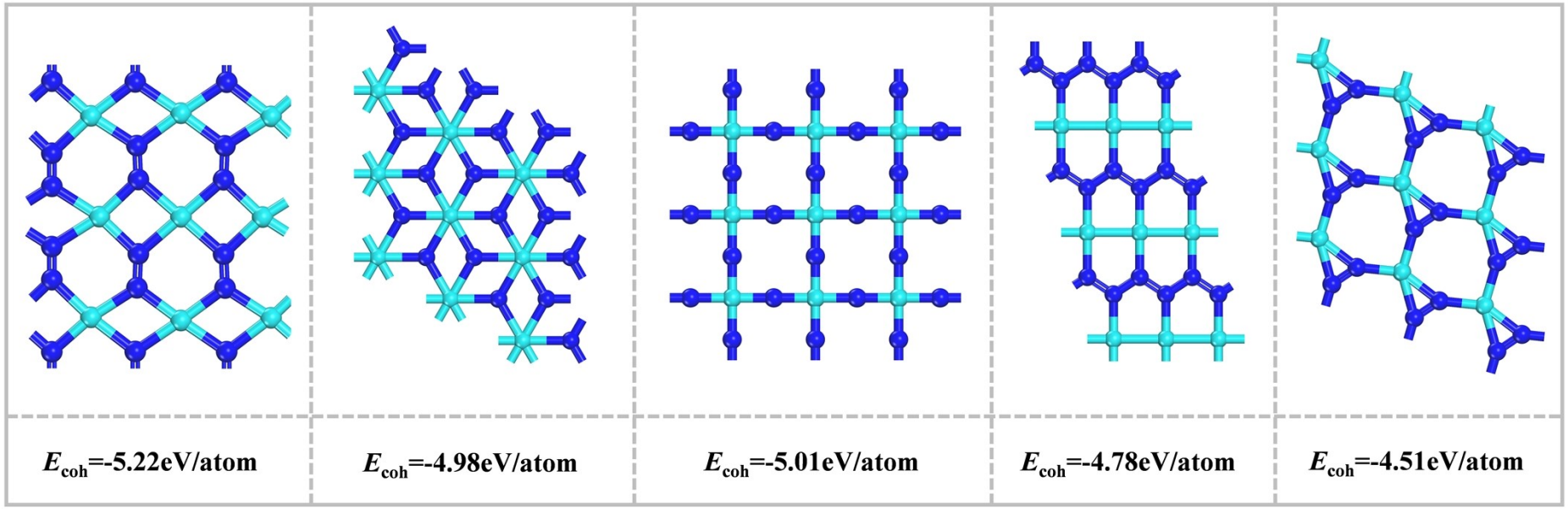

Fig. S4 Low-lying isomers of the IrN_2 monolayer. The values denote the cohesive energy (E_{coh}) of the corresponding structures.

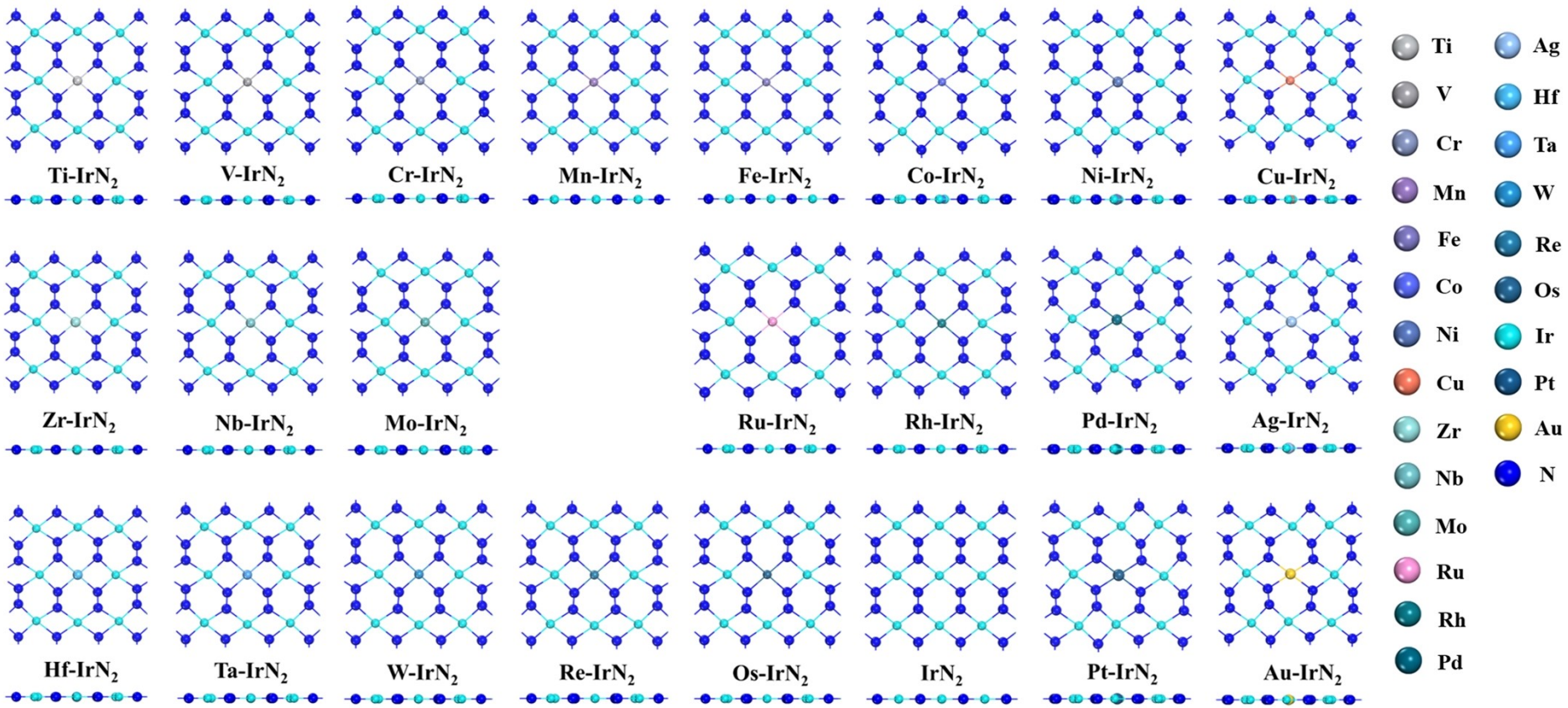

Fig. S5 Optimized geometric structure of IrN_2/TM-IrN_2.

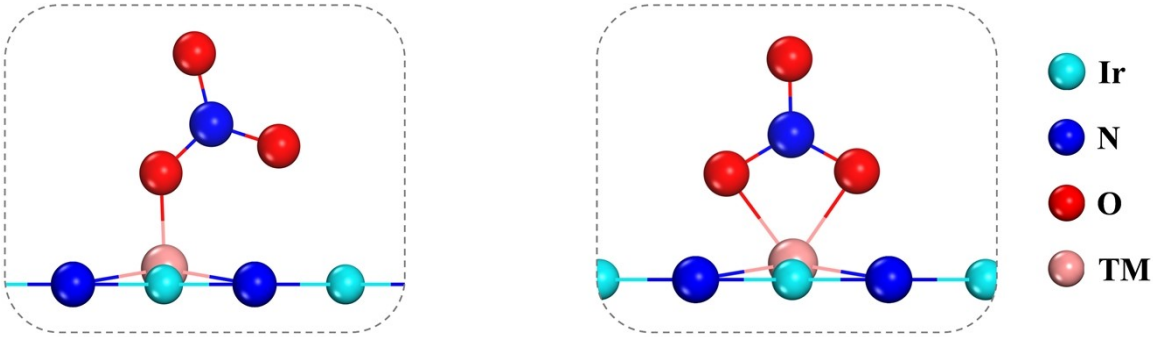

Fig. S6 NO_3^- adsorption configurations: (Left) the 1-O configuration (one oxygen atom adsorbed on TM-IrN_2) and (right) the 2-O configuration (two oxygen atoms adsorbed on TM-IrN_2).

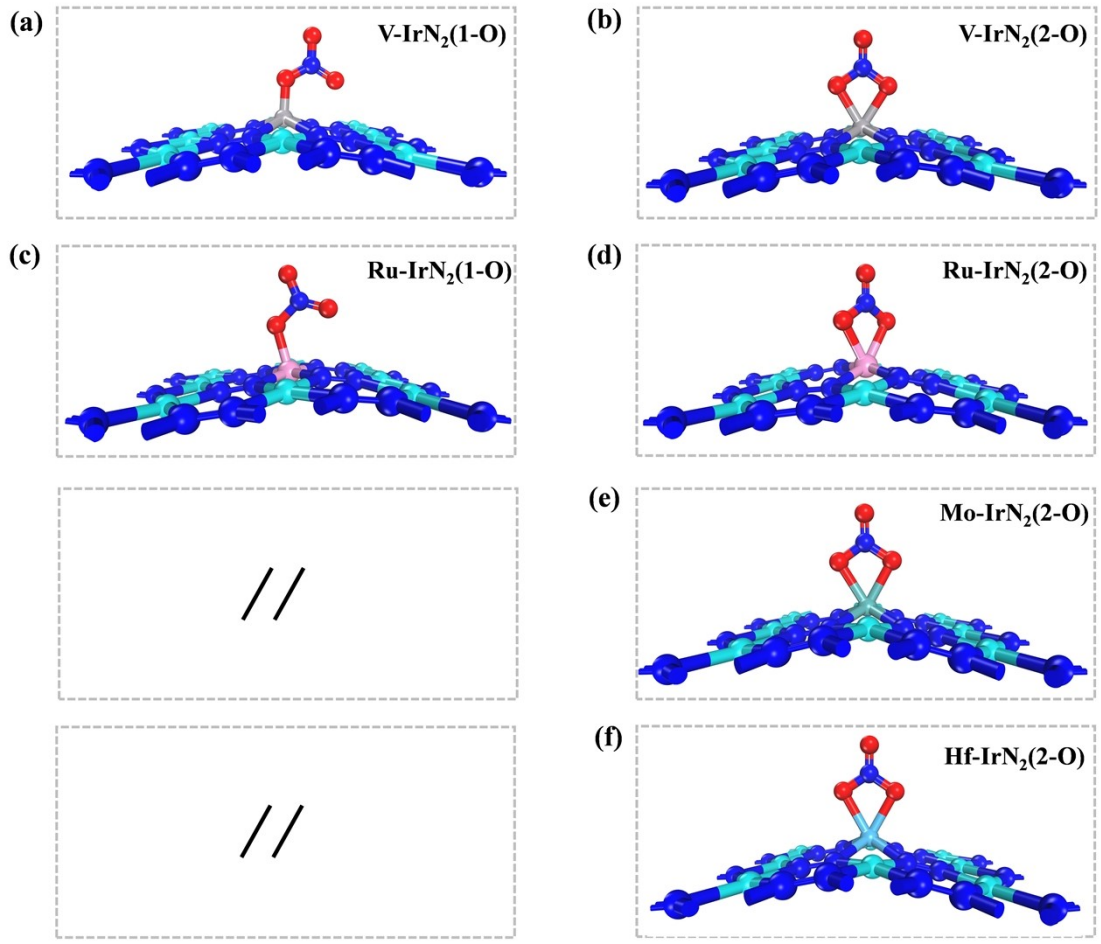

Fig. S7 (a) The 1-O adsorption configuration of NO_3^- on V-IrN_2. (b) The 2-O adsorption configuration of NO_3^- on V-IrN_2. (c) The 1-O adsorption configuration of NO_3^- on Ru-IrN_2. (d) The 2-O adsorption configuration of NO_3^- on Ru-IrN_2. (e) The 2-O adsorption configuration of NO_3^- on Mo-IrN_2. (f) The 2-O adsorption configuration of NO_3^- on Hf-IrN_2. "//" indicates that the 1-O adsorption mode does not exist for Mo-IrN_2 and Hf-IrN_2.

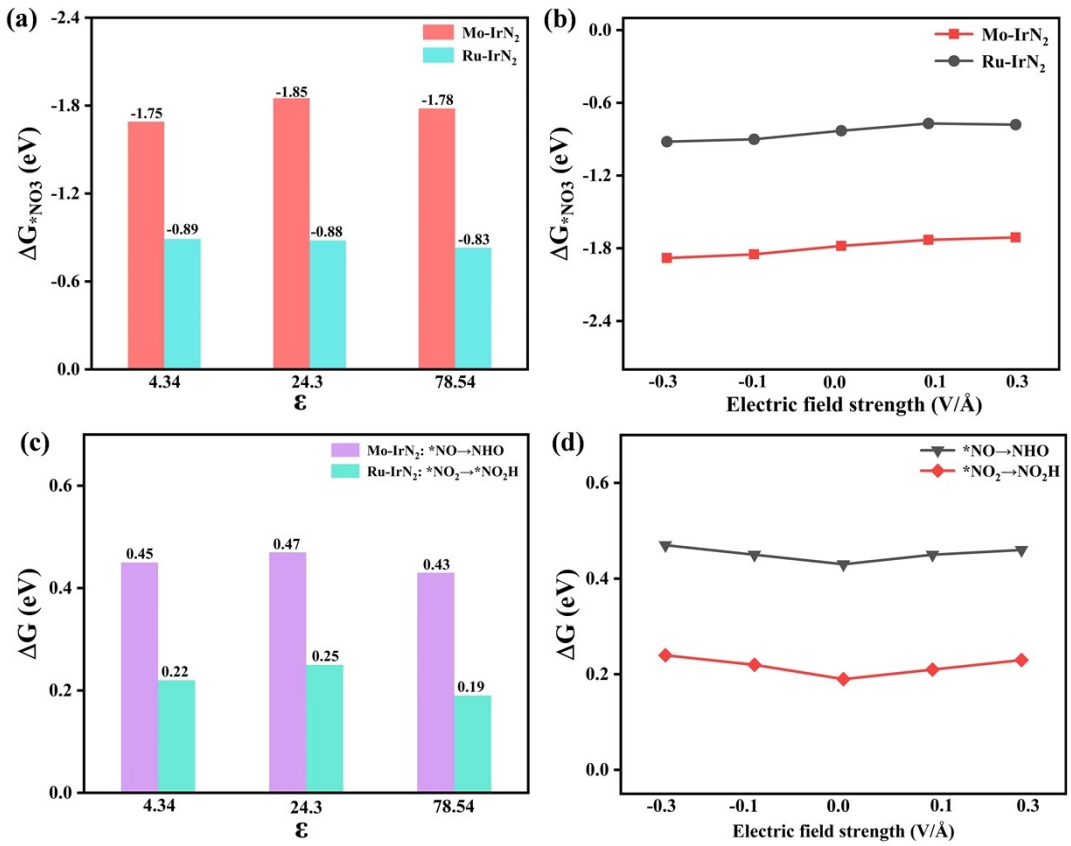

Fig. S8 (a) ΔG_{*NO_3} values for Mo-IrN_2 and Ru-IrN_2 at different dielectric constants (ε). (b) Variation of ΔG_{*NO_3} as a function of electric field strength for Mo-IrN_2 and Ru-IrN_2 catalysts. (c) ΔG_{PDS} values for Mo-IrN_2 and Ru-IrN_2 at different dielectric constants (ε). (d) Variation of ΔG_{PDS} as a function of electric field strength for Mo-IrN_2 and Ru-IrN_2 catalysts.

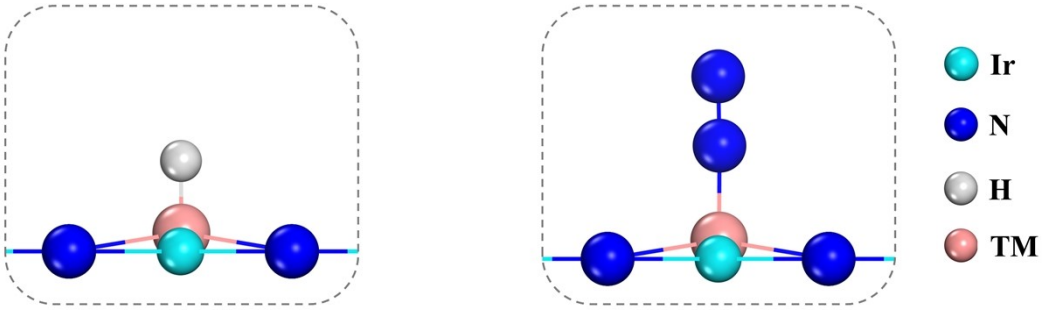

Fig. S9 Schematic diagram of the configuration of H protons and N_2 molecules adsorbed on TM-IrN_2

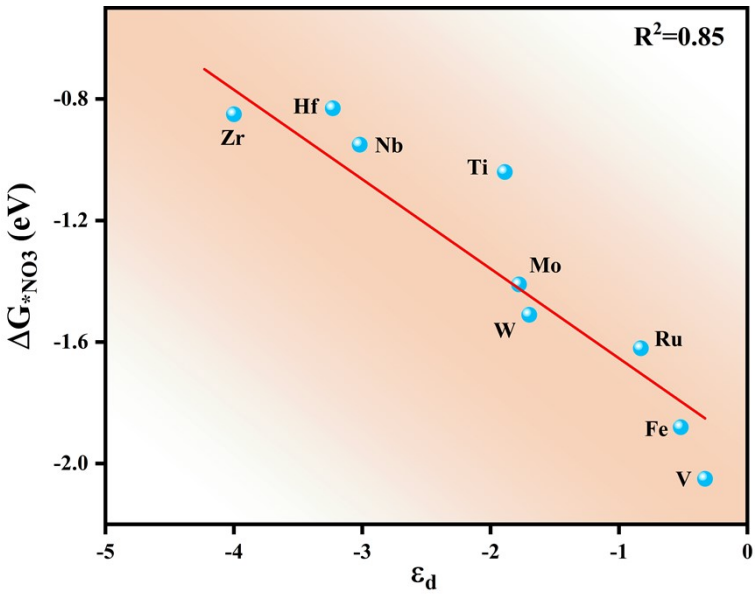

Fig. S10. Relationship between d-band center (ε_d) and *NO_3 adsorption free energy (ΔG_{*NO_3}).

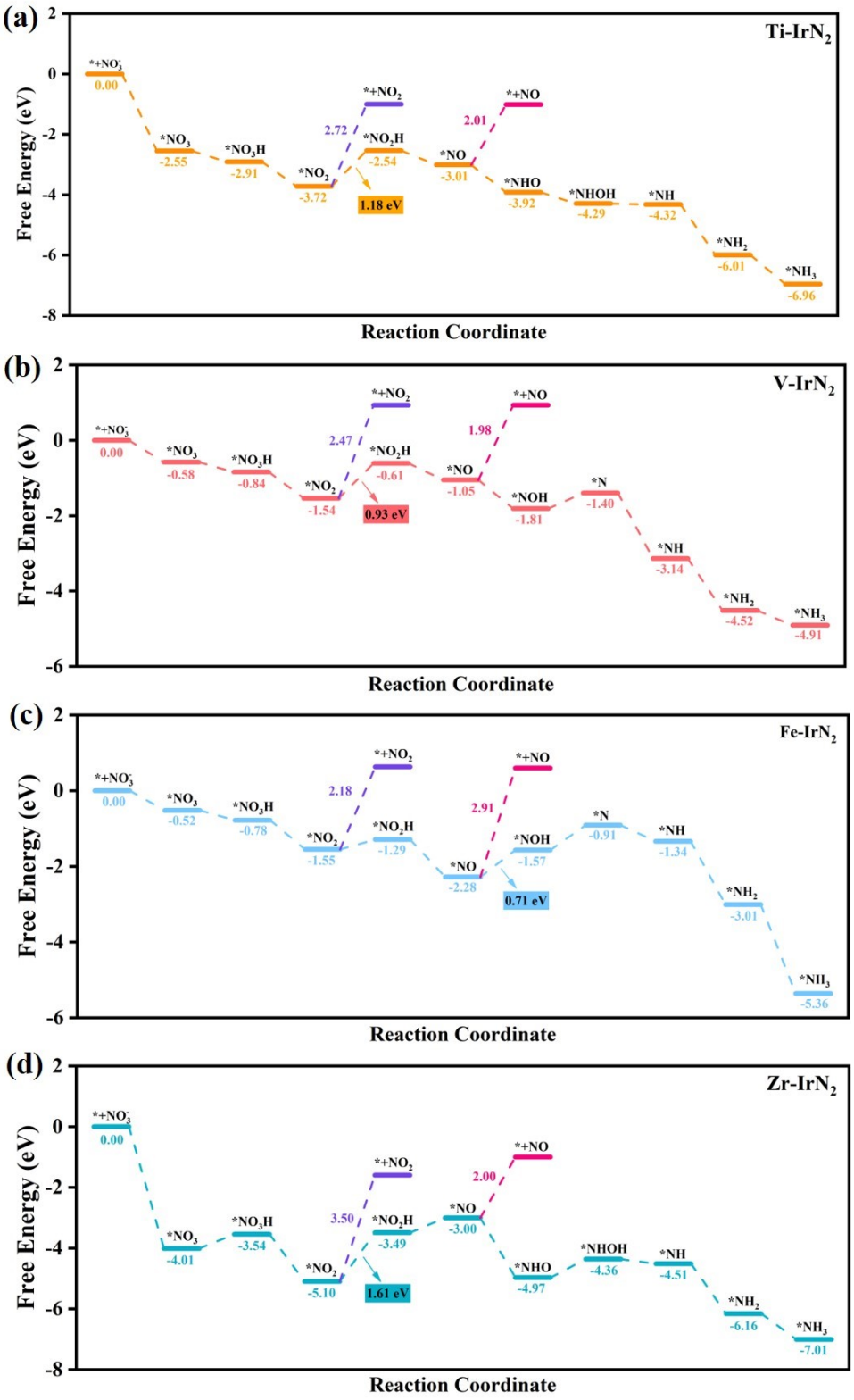

Fig. S11 Free energy diagrams of the optimal NO_3RR pathway on (a) Ti-IrN_2, (b) V-IrN_2, (c) Fe-IrN_2 and (d) Zr-IrN_2.

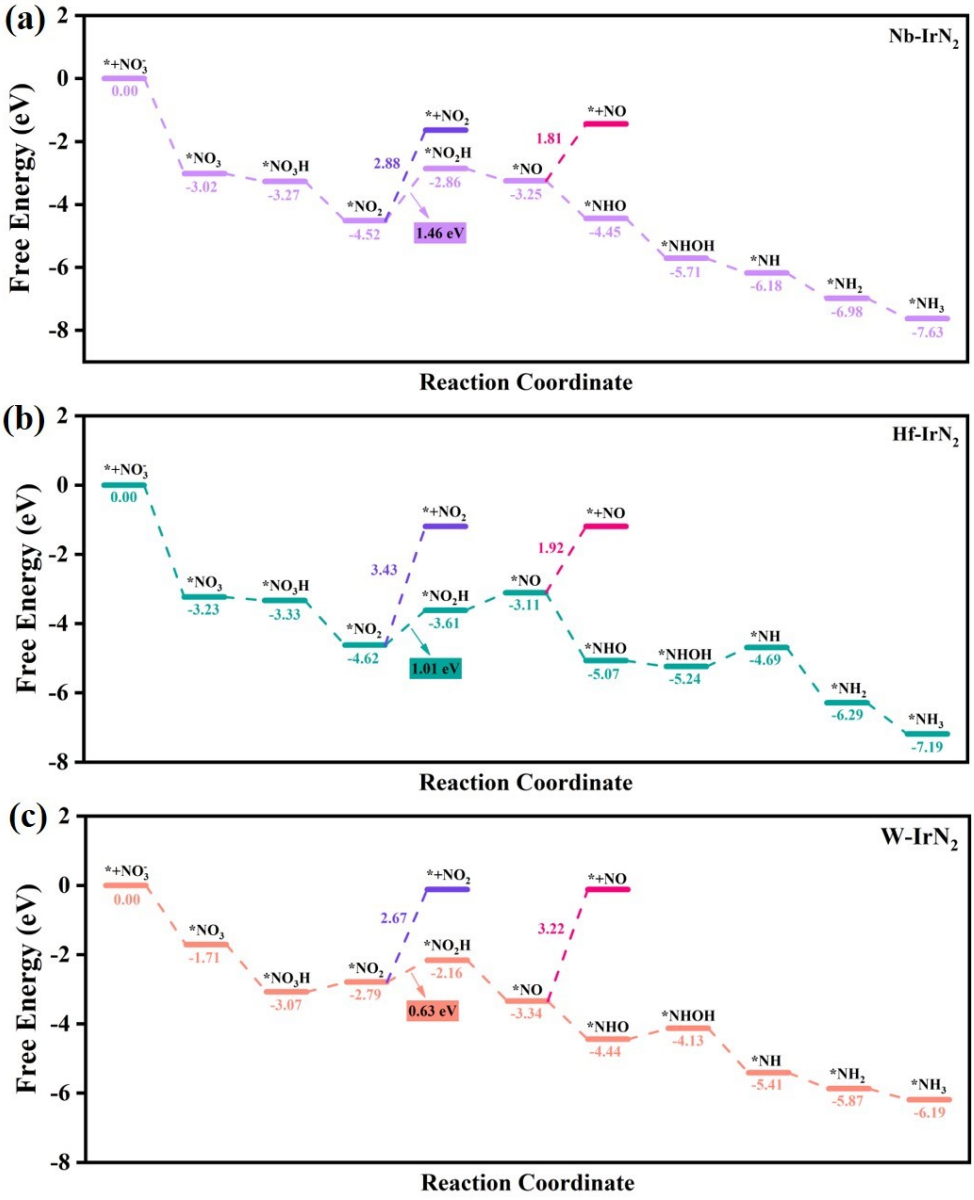

Fig. S12 Free energy diagrams of the optimal NO_3RR pathway on (a) Nb-IrN_2, (b) Hf-IrN_2 and (c) W-IrN_2.

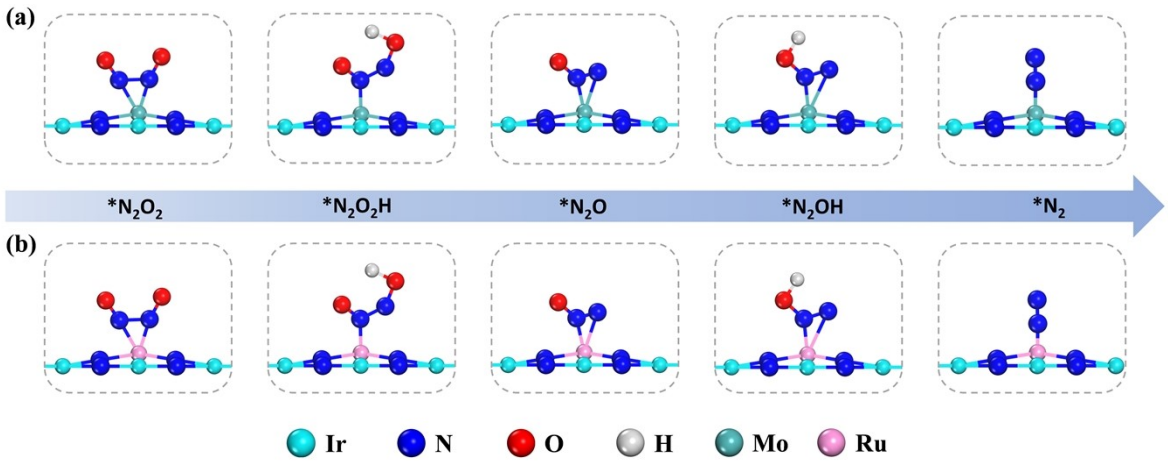

Fig. S13 The optimal structures of each intermediates product for byproduct-N_2 synthesis.

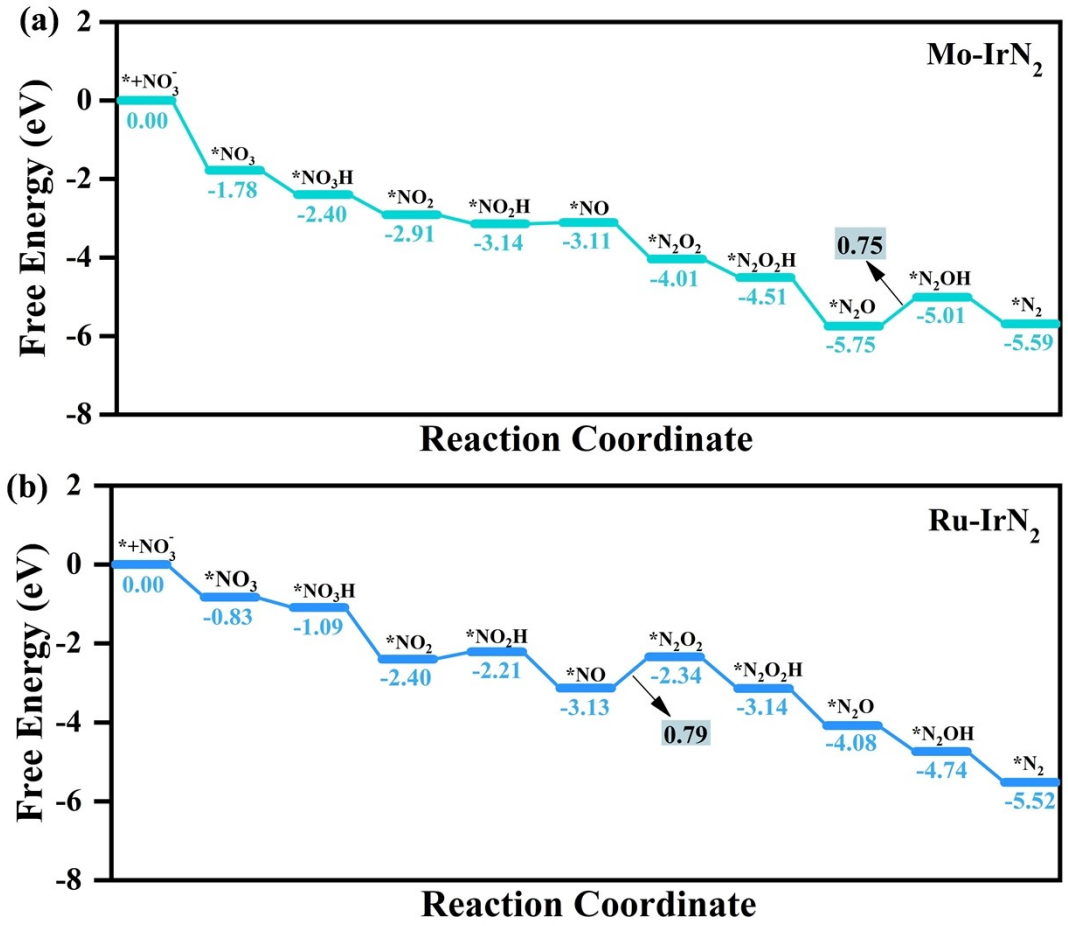

Fig. S14 Free energy diagrams of the reaction paths for the generation of N_2 on (a) Mo-IrN_2 and (b) Ru-IrN_2.

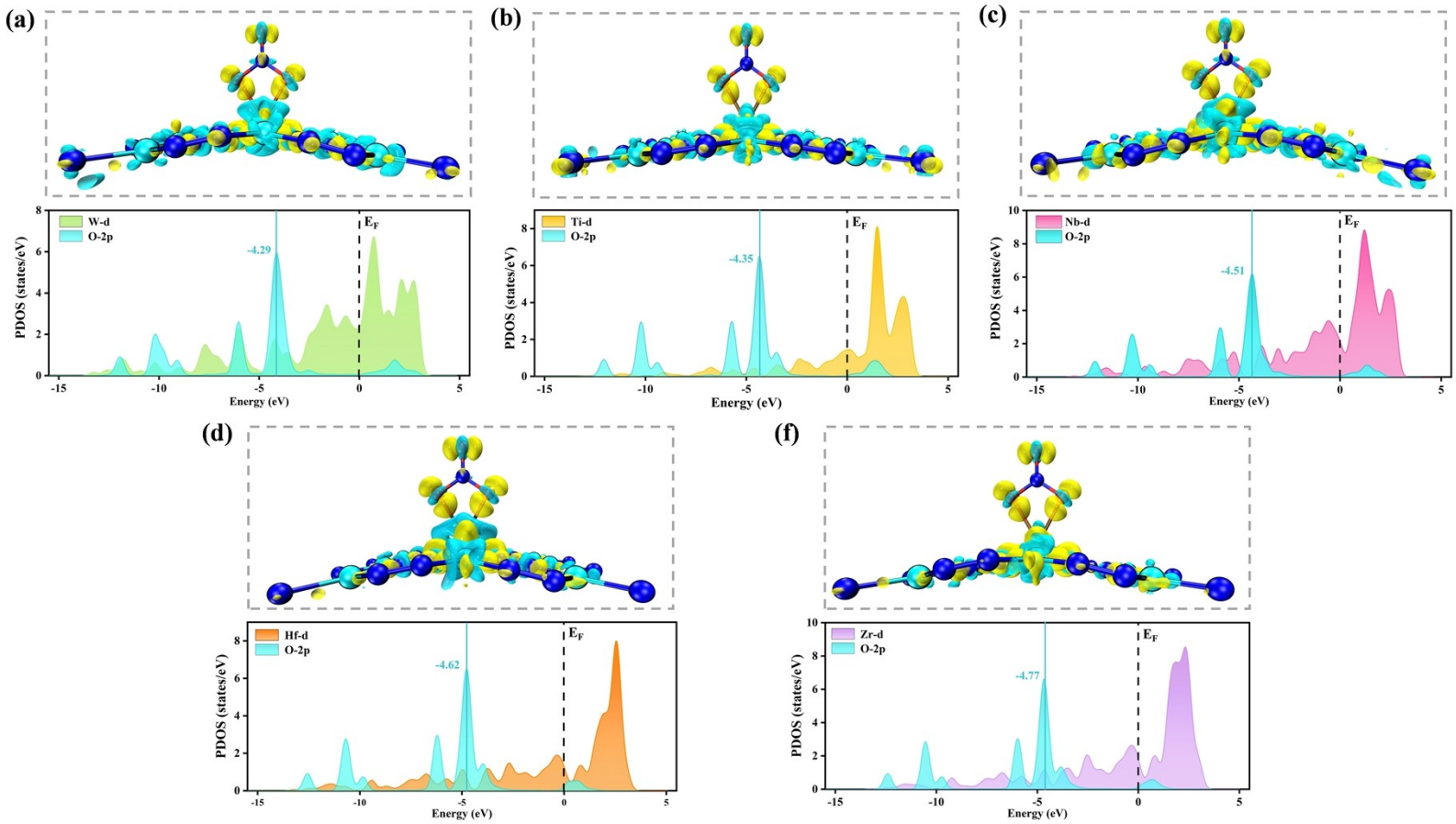

Fig. S15 Charge density difference and PDOS of $^{NO_3^-}$ on (a) W-IrN_2, (b) Ti-IrN_2, (c) Nb-IrN_2, (d) Hf-IrN_2, and (e) Zr-IrN_2. Yellow isosurfaces represent electron accumulation; blue denotes electron depletion.

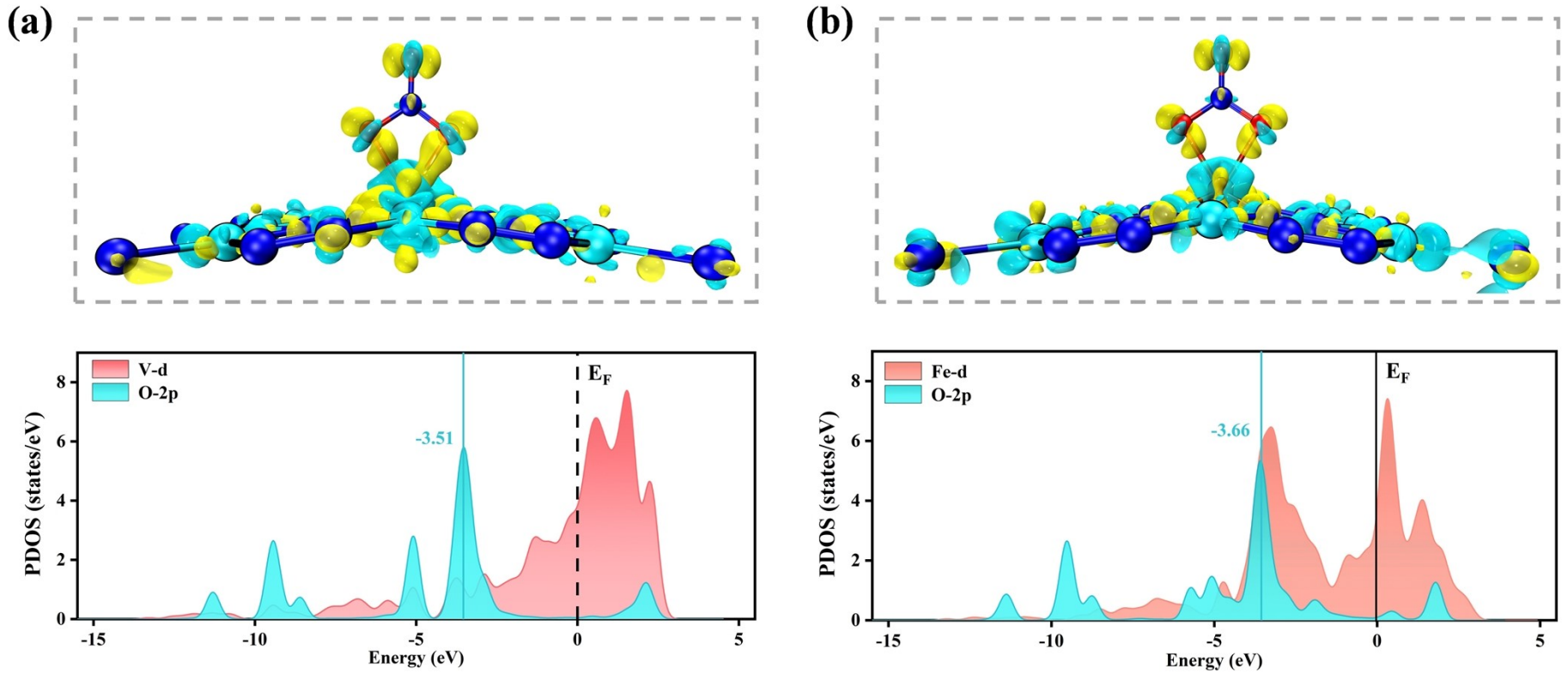

Fig. S16 Charge density difference and PDOS of $^{NO_3^-}$ on (a) V-IrN_2 and (b) Fe-IrN_2. Yellow isosurfaces represent electron accumulation; blue denotes electron depletion.

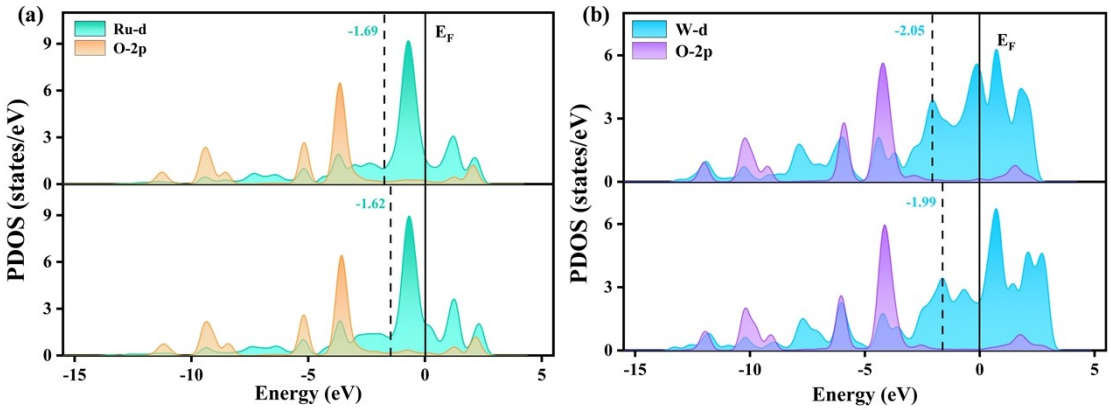

Fig. S17 PDOSs of NO_3-adsorbed (a) Ru-IrN_2 and (b) W-IrN_2. The solid line denotes the Fermi level, and the dashed line represents the d-band center. The top and bottom panels show the all-electron and scalar relativistic DSPP calculations, respectively.

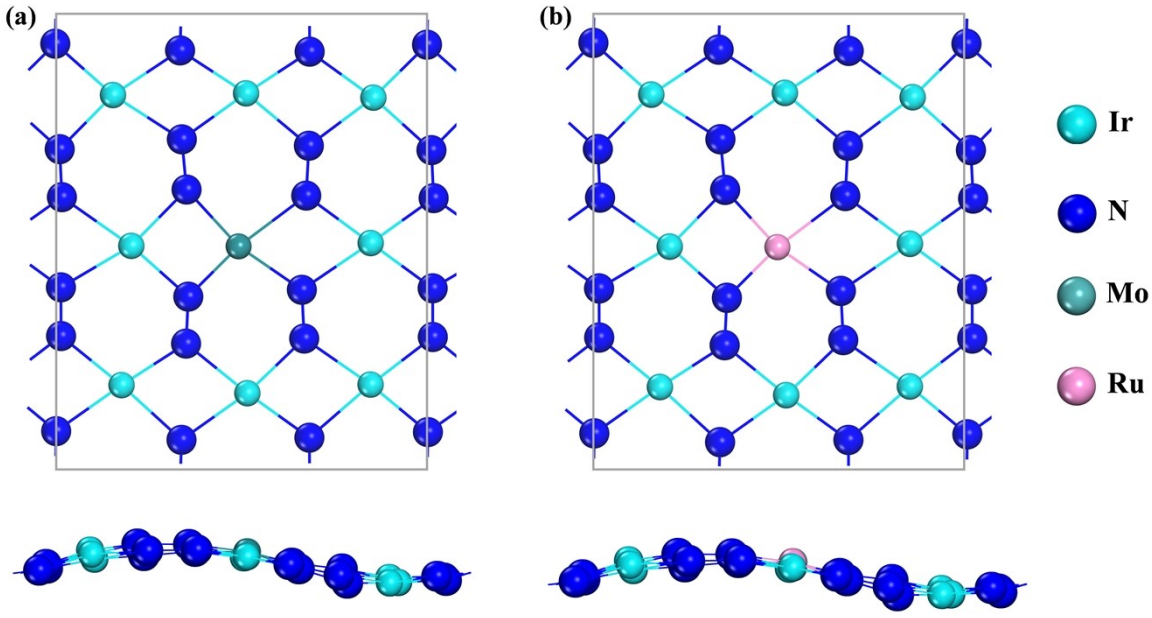

Fig. S18 The completely optimized model after AIMD of (a) Mo-IrN_2 and (b) Ru-IrN_2. The top and side view are also displayed.

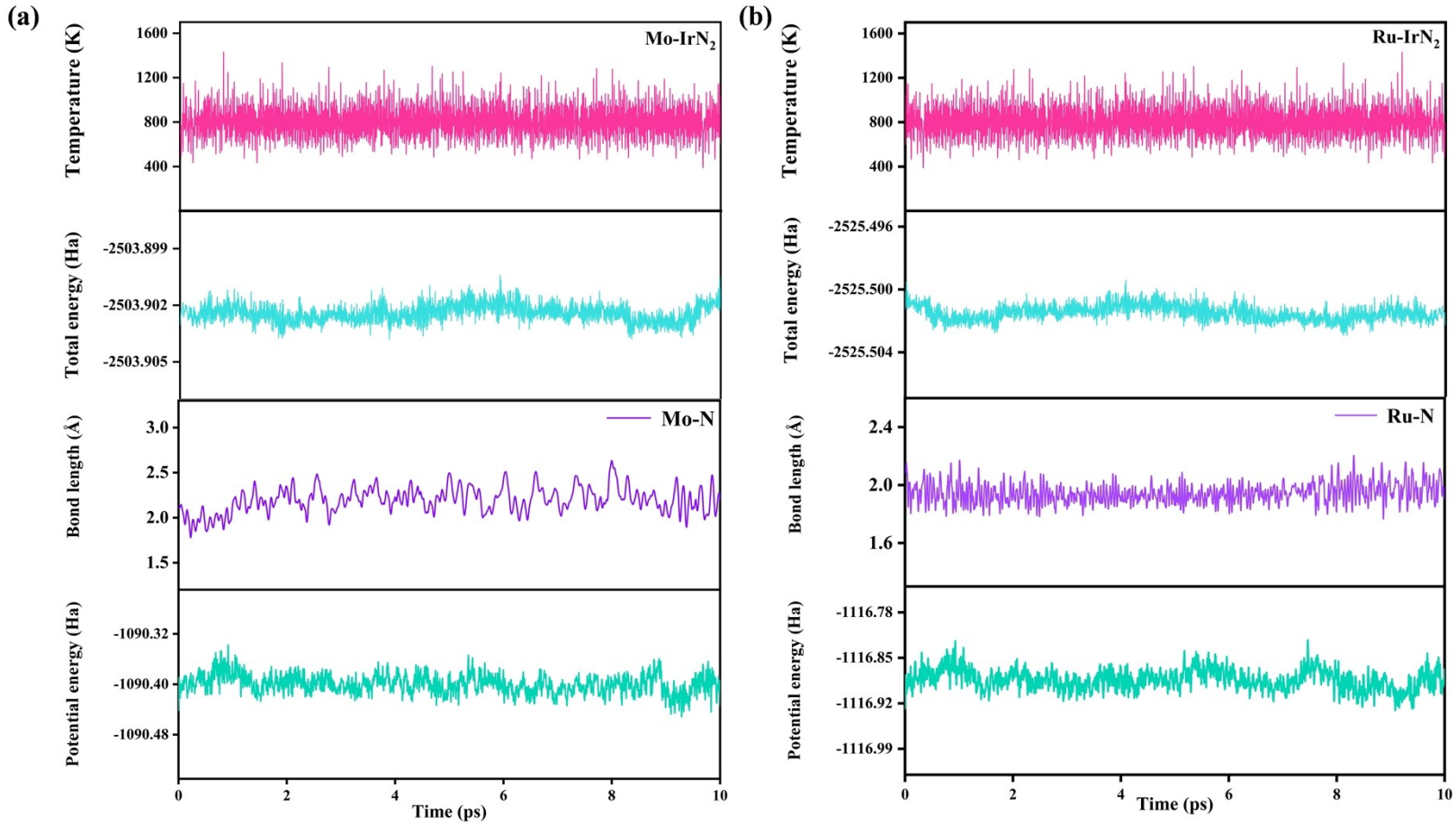

Fig. S19 Evolution of temperature, total energy, potential energy, and TM-N bond length versus AIMD time for (a) Mo-IrN_2 and (b) Ru-IrN_2. The AIMD simulation lasted 10 ps at 800 K.

Table S1. Lattice constants *a/b*, bond lengths *d* (in Å) and cohesion energy E_{coh} (in eV atom^{-1}) of IrN_2. The bright blue and dark blue balls represent Ir and N atoms, respectively.

Structure	Parameters	This work	Reference 1	Graphic
Unit cell	a	3.196	3.20	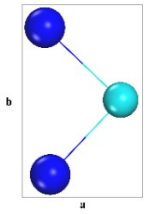
	b	3.717	3.72	
Monolayer	$d_{Ir\text{-}N}$	2.003	1.99	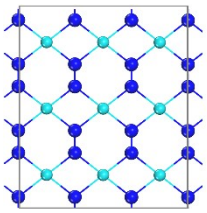
	$d_{N\text{-}N}$	1.223	1.22	
	E_{coh}	5.22	5.24	

Table S2. Calculated bond lengths d (in Å) and TM adsorption energies ΔE_{TM} (in eV) for IrN_2 and TM-IrN_2.

Catalysts	d_{TM-N}	d_{N-N}	ΔE_{TM}
IrN_2	2.003	1.223	-5.61
Ti-IrN_2	2.009	1.230	-5.85
V-IrN_2	2.028	1.248	-6.37
Cr-IrN_2	2.012	1.231	-3.44
Mn-IrN_2	2.028	1.264	-4.57
Fe-IrN_2	2.030	1.265	-4.89
Co-IrN_2	2.081	1.265	-5.26
Ni-IrN_2	2.078	1.265	-5.28
Cu-IrN_2	2.051	1.246	-3.03
Zr-IrN_2	1.998	1.235	-6.47
Nb-IrN_2	2.008	1.228	-5.46
Mo-IrN_2	2.011	1.227	-4.13
Ru-IrN_2	2.023	1.226	-4.39
Rh-IrN_2	2.023	1.229	-4.10
Pd-IrN_2	2.066	1.243	-3.13
Ag-IrN_2	2.048	1.242	-1.49
Hf-IrN_2	1.995	1.235	-6.30
Ta-IrN_2	2.006	1.230	-6.48
W-IrN_2	2.015	1.237	-6.26
Re-IrN_2	2.016	1.225	-4.39
Os-IrN_2	2.026	1.237	-5.41
Pt-IrN_2	2.059	1.244	-4.67
Au-IrN_2	2.044	1.244	-1.98

Table S3. Work function (in eV) and Hirshfeld charge (in |e|) for IrN_2 and TM-IrN_2.

Catalysts	Work function	q_{TM}	$q_{ortho\text{-}Ir}$	$q_{ortho\text{-}N}$
IrN_2	6.09	0.163	0.163	-0.081
Ti-IrN_2	5.66	0.586	0.105	-0.135
V-IrN_2	5.77	0.394	0.131	-0.115
Cr-IrN_2	5.82	0.484	0.115	-0.121
Mn-IrN_2	5.74	0.391	0.139	-0.109
Fe-IrN_2	5.82	0.193	0.133	-0.074
Co-IrN_2	5.80	0.187	0.131	-0.080
Ni-IrN_2	5.82	0.101	0.138	-0.068
Cu-IrN_2	5.85	0.338	0.123	-0.101
Zr-IrN_2	5.60	0.756	0.092	-0.152
Nb-IrN_2	5.74	0.658	0.092	-0.152
Mo-IrN_2	5.76	0.531	0.099	-0.124
Ru-IrN_2	5.82	0.351	0.117	-0.092
Rh-IrN_2	5.80	0.247	0.127	-0.077
Pd-IrN_2	6.04	0.382	0.121	-0.117
Ag-IrN_2	5.79	0.370	0.122	-0.100
Hf-IrN_2	5.65	0.658	0.103	-0.145
Ta-IrN_2	5.82	0.564	0.099	-0.137
W-IrN_2	5.82	0.484	0.108	-0.121
Re-IrN_2	5.87	0.395	0.105	-0.100
Os-IrN_2	5.80	0.287	0.121	-0.096
Pt-IrN_2	6.04	0.215	0.134	-0.093
Au-IrN_2	5.87	0.366	0.119	-0.098

Table S4. Formation energy E_f (in eV), dissolution potential U_{diss} (in V), standard dissolution potential (U_{diss}^{0}) of metal, and number of transferred electrons (n) during the dissolution for IrN_2 and TM-IrN_2.

Catalysts	E_f	n	U_{diss}^{0}	U_{diss}
IrN_2	-1.48	3	1.16	1.65
Ti-IrN_2	-3.32	2	-1.63	0.03
V-IrN_2	-2.60	2	-1.18	0.12
Cr-IrN_2	0.26	2	-0.91	-1.04
Mn-IrN_2	-2.53	2	-1.19	0.07
Fe-IrN_2	-1.25	2	-0.45	0.18
Co-IrN_2	-1.84	2	-0.28	0.64
Ni-IrN_2	-2.14	2	-0.26	0.81
Cu-IrN_2	-1.57	2	0.34	1.12
Zr-IrN_2	-6.43	4	-1.45	0.16
Nb-IrN_2	-3.55	3	-1.10	0.08
Mo-IrN_2	-1.22	3	-0.2	0.21
Ru-IrN_2	-0.75	2	0.46	0.83
Rh-IrN_2	0.80	2	0.60	0.2
Pd-IrN_2	-1.02	2	0.95	1.46
Ag-IrN_2	-0.87	1	0.80	1.67
Hf-IrN_2	-6.59	4	-1.55	0.09
Ta-IrN_2	0.86	3	-0.6	-0.89
W-IrN_2	-0.96	3	0.1	0.42
Re-IrN_2	1.61	3	0.3	-0.24
Os-IrN_2	-0.34	8	0.84	0.88
Pt-IrN_2	-1.58	2	1.18	1.97
Au-IrN_2	-1.08	3	1.50	1.86

Note: All the U_{diss}^{0} and n values refer to those in Ref. 2.

Table S5. Gibbs free energy of adsorption of NO_3^- on IrN_2 and TM-IrN_2 with different adsorption modes.

Catalysts	ΔG_{*NO_3} /1-O pattern	ΔG_{*NO_3} /2-O pattern
IrN_2	0.54	//
Ti-IrN_2	//	-1.89
V-IrN_2	0.72	-0.33
Mn-IrN_2	//	0.55
Fe-IrN_2	//	-0.52
Co-IrN_2	1.23	1.24
Ni-IrN_2	1.75	//
Cu-IrN_2	1.25	0.85
Zr-IrN_2	//	-4.00
Nb-IrN_2	//	-3.02
Mo-IrN_2	//	-1.78
Ru-IrN_2	-0.32	-0.83
Pd-IrN_2	0.72	//
Ag-IrN_2	1.30	0.86
Hf-IrN_2	//	-3.23
W-IrN_2	//	-1.70
Os-IrN_2	0.13	0.17
Pt-IrN_2	1.49	//
Au-IrN_2	//	1.52

Note: // indicates that the corresponding NO_3^- adsorption mode does not exist.

Table S6. Calculated Gibbs free energy *G* and its electronic *E*, zero-point ZPE, and entropic contributions TS (in eV) involved in the NO_3^- adsorption on V-IrN_2, Ru-IrN_2, Mo-IrN_2, and Hf-IrN_2.

Structure	Adsorption mode	Species	*E*	ZPE	TS	*G*	ΔG_{*NO_3}
V-IrN_2	1-O	*NO_3	-75507.59	0.54	0.13	-75507.18	0.72
		*	-67883.99	0.79	0.53	-67883.73	
		HNO_3	-7639.78	0.69	0.60	-7639.69	
		H_2	-31.68	0.27	0.42	-31.83	
V-IrN_2	2-O	*NO_3	-75508.65	0.55	0.13	-75508.23	-0.33
		*	-67883.99	0.79	0.53	-67883.73	
		HNO_3	-7639.78	0.69	0.60	-7639.69	
		H_2	-31.68	0.27	0.42	-31.83	
Ru-IrN_2	1-O	*NO_3	-76589.12	0.45	0.13	-76588.80	-0.32
		*	-68964.67	0.89	0.53	-68964.31	
		HNO_3	-7639.78	0.69	0.60	-7639.69	
		H_2	-31.68	0.27	0.42	-31.83	
Ru-IrN_2	2-O	*NO_3	-76589.58	0.40	0.13	-76589.31	-0.83
		*	-68964.67	0.89	0.53	-68964.31	
		HNO_3	-7639.78	0.69	0.60	-7639.69	
		H_2	-31.68	0.27	0.42	-31.83	
Mo-IrN_2	2-O	*NO_3	-75762.89	0.43	0.18	-75762.64	-1.78
		*	-68137.05	0.90	0.54	-68136.69	
		HNO_3	-7639.78	0.69	0.60	-7639.69	
		H_2	-31.68	0.27	0.42	-31.83	
Hf-IrN_2	2-O	*NO_3	-76288.26	0.64	0.11	-76287.73	-3.23
		*	-68660.58	0.70	0.45	-68660.33	
		HNO_3	-7639.78	0.69	0.60	-7639.69	
		H_2	-31.68	0.27	0.42	-31.83	

Table S7. Gibbs free energy of NO_3^- adsorption ΔG_{*NO_3} (in eV) and U_L (in V) values on TM-IrN_2.

Catalysts	ΔG_{*NO_3}	U_L
Ti-IrN_2	-1.89	-1.18
V-IrN_2	-0.33	-0.93
Fe-IrN_2	-0.52	-0.71
Zr-IrN_2	-4.00	-1.61
Nb-IrN_2	-3.02	-1.46
Mo-IrN_2	-1.78	-0.43
Ru-IrN_2	-0.83	-0.19
Hf-IrN_2	-3.23	-1.01
W-IrN_2	-1.70	-0.62

Note: Uncertainties are estimated as ±0.05–0.10 eV for ΔG_{*NO_3} and ±0.05–0.10 V for U_L.

Table S8. Calculated Gibbs free energy *G* and its electronic *E*, zero-point ZPE, and entropic contributions TS (in eV) involved in potential-determining steps on Mo-IrN_2 and Ru-IrN_2.

Structure	Species	*E*	ZPE	TS	*G*	Δ*G*
Mo-IrN_2	*NO	-71687.86	0.45	0.17	-71687.58	0.43
	*NHO	-71672.12	0.16	0.13	-71672.09	
Ru-IrN_2	*NO_2	-74560.03	0.61	0.23	-74559.65	0.19
	*NO_2H	-74544.10	0.33	0.15	-74543.92	

Table S9. Calculated Gibbs free energy *G* and its electronic *E*, zero-point ZPE, and entropic contributions TS (in eV) involved in *H adsorption on Mo-IrN_2 and Ru-IrN_2.

Structure	Species	*E*	ZPE	TS	*G*	ΔG_{*H}
Mo-IrN_2	*H	-68153.70	0.18	0.02	-68153.54	-0.94
	*	-68137.05	0.90	0.54	-68136.69	
	H_2	-31.68	0.27	0.42	-31.83	
Ru-IrN_2	*H	-68981.12	0.20	0.02	-68980.94	-0.72
	*	-68964.67	0.89	0.53	-68964.31	
	H_2	-31.68	0.27	0.42	-31.83	

The structural file for Mo-IrN_2

Mo-IrN_2

1.0

9.5867996216	0.0000000000	0.0000000000
-0.0290030500	11.2661627337	0.0000000000
0.0000000000	0.0000000000	15.0082998276

Ir	N	Mo
8	18	1

Direct

0.266959995	0.171599999	0.000290000
0.615649998	0.161809996	0.000290000
0.964280009	0.171409994	0.000290000
0.299640000	0.503090024	0.000290000
0.931550026	0.503229976	0.000290000
0.266909987	0.834909976	0.000290000
0.615540028	0.844500005	0.000290000
0.964230001	0.834720016	0.000290000
0.115659997	0.294939995	0.000290000
0.115470000	0.057519998	0.000290000
0.445279986	0.269010007	0.000290000
0.438520014	0.059429999	0.000290000
0.786300004	0.269030005	0.000290000
0.792599976	0.059360001	0.000290000
0.115699999	0.602429986	0.000290000
0.115489997	0.403890014	0.000290000
0.450670004	0.625519991	0.000290000
0.450610012	0.380840003	0.000290000
0.780579984	0.625479996	0.000290000
0.780520022	0.380800009	0.000290000
0.115719996	0.948800027	0.000290000
0.115529999	0.711369991	0.000290000
0.438589990	0.946959972	0.000290000
0.444889992	0.737280011	0.000290000
0.792670012	0.946889997	0.000290000
0.785910010	0.737299979	0.000290000
0.615599990	0.503160000	0.000290000

The structural file for Ru-IrN_2

Ru-IrN_2

1.0

9.5867996216	0.0000000000	0.0000000000
-0.0290030500	11.2661627337	0.0000000000
0.0000000000	0.0000000000	15.0082998276

Ir	N	Ru
8	18	1

Direct

0.268070012	0.171279997	0.000290000
0.615599990	0.162560001	0.000290000
0.963240027	0.171090007	0.000290000
0.300850004	0.503080010	0.000290000
0.930339992	0.503239989	0.000290000
0.267949998	0.835229993	0.000290000
0.615599990	0.843760014	0.000290000
0.963119984	0.835039973	0.000290000
0.115699999	0.295139998	0.000290000
0.115500003	0.057870001	0.000290000
0.446469992	0.271620005	0.000290000
0.439590007	0.059549998	0.000290000
0.785059988	0.271580011	0.000290000
0.791570008	0.059500001	0.000290000
0.115709998	0.602320015	0.000290000
0.115479998	0.404000014	0.000290000
0.451539993	0.623830020	0.000290000
0.451510012	0.382589996	0.000290000
0.779680014	0.623719990	0.000290000
0.779649973	0.382490009	0.000290000
0.115690000	0.948450029	0.000290000
0.115489997	0.711170018	0.000290000
0.439619988	0.946810007	0.000290000
0.446130008	0.734730005	0.000290000
0.791599989	0.946770012	0.000290000
0.784720004	0.734700024	0.000290000
0.615599990	0.503160000	0.000290000

The structural file for Mo-IrN_2-*NO_3

Mo-IrN_2-*NO_3

1.0

9.5867996216	0.0000000000	0.0000000000
-0.0290030500	11.2661627337	0.0000000000
0.0000000000	0.0000000000	15.0082998276

Ir	N	Mo	O
8	19	1	3

Direct

0.284969985	0.174750000	0.976589978
0.616360009	0.164189994	0.975650012
0.947619975	0.174789995	0.976580024
0.298449993	0.499810010	0.020780001
0.934279978	0.499870002	0.020880001
0.263190001	0.834110022	0.980560005
0.616259992	0.837450027	0.980520010
0.969269991	0.833819985	0.980509996
0.116360001	0.285089999	0.991219997
0.116090000	0.067879997	0.970009983
0.455969989	0.277539998	0.986259997
0.444929987	0.055210002	0.971809983
0.776899993	0.277619988	0.986289978
0.787590027	0.055140000	0.971740007
0.116410002	0.602760017	0.020900000
0.116379999	0.393180013	0.013470000
0.449829996	0.619629979	0.002780000
0.459259987	0.387730002	0.002500000
0.782739997	0.619480014	0.002780000
0.773429990	0.387760013	0.002590000
0.116250001	0.957449973	0.971700013
0.116279997	0.710049987	0.001640000
0.441810012	0.943090022	0.973299980
0.446009994	0.729709983	0.989929974
0.790790021	0.943069994	0.973240018
0.786300004	0.729640007	0.989939988
0.616219997	0.510890007	0.219540000
0.616320014	0.502839983	0.046399999
0.616169989	0.513149977	0.299450010
0.616299987	0.604870021	0.167750001
0.616180003	0.413239986	0.171189994

The structural file for Ru-IrN_2-*NO_3

Ru-IrN_2-*NO_3

1.0

9.5867996216	0.0000000000	0.0000000000
-0.0290030500	11.2661627337	0.0000000000
0.0000000000	0.0000000000	15.0082998276

Ir	N	Ru	O
8	19	1	3

Direct

0.303209990	0.164470002	0.985210001
0.594959974	0.175840005	0.988439977
0.949039996	0.171519995	0.978479981
0.262149990	0.507369995	0.007710000
0.970330000	0.499220014	0.007510000
0.283419997	0.835009992	0.977680027
0.637430012	0.830680013	0.987600029
0.929300010	0.842060030	0.984340012
0.126859993	0.269129992	0.990119994
0.118380003	0.059260000	0.977699995
0.443100005	0.293729991	0.005780000
0.454970002	0.045260001	0.978640020
0.777149975	0.283369988	0.989989996
0.771579981	0.071539998	0.974940002
0.111019999	0.627590001	0.998099983
0.121490002	0.378899992	0.998920023
0.447519988	0.612410009	0.995700002
0.433899999	0.401100010	0.021520000
0.798460007	0.605430007	0.020360000
0.784979999	0.394059986	0.996219993
0.114150003	0.947309971	0.977339983
0.105650000	0.737330019	0.989049971
0.460850000	0.935029984	0.974600017
0.455269992	0.723039985	0.989139974
0.777480006	0.961279988	0.978410006
0.789330006	0.712800026	0.004550000
0.616609991	0.504450023	0.210069999
0.616509974	0.503459990	0.038210001
0.616819978	0.504840016	0.290479988
0.552039981	0.582589984	0.160689995
0.680989981	0.425729990	0.161019996

The structural file for Mo-IrN$_2$-*NO

Mo-IrN$_2$-*NO

1.0

9.5867996216	0.0000000000	0.0000000000
-0.0290030500	11.2661627337	0.0000000000
0.0000000000	0.0000000000	15.0082998276

Ir	N	Mo	O
8	19	1	1

Direct

0.301880002	0.177819997	0.974359989
0.596790016	0.168119997	0.977209985
0.948729992	0.174229994	0.970780015
0.282819986	0.505119979	0.018810000
0.932190001	0.498930007	0.015969999
0.259279996	0.833329976	0.987909973
0.616559982	0.838440001	0.986090004
0.967060030	0.841579974	0.985800028
0.118680000	0.283829987	0.985220015
0.125149995	0.072549999	0.967149973
0.454140007	0.295769989	0.991419971
0.443470001	0.047649998	0.972050011
0.773620009	0.272870004	0.983770013
0.780499995	0.061129998	0.969969988
0.106610000	0.605379999	0.018660000
0.114399999	0.392390013	0.006260000
0.445279986	0.620180011	0.014070000
0.454329997	0.403290004	0.008880000
0.786059976	0.627629995	0.013260000
0.777369976	0.381559998	0.000920000
0.119599998	0.962880015	0.973630011
0.109540001	0.714649975	0.005060000
0.437920004	0.937579989	0.975570023
0.444480002	0.729610026	0.999539971
0.784910023	0.949289978	0.974820018
0.790040016	0.738229990	0.998849988
0.598959982	0.510950029	0.173820004
0.637589991	0.505800009	0.048710000
0.660160005	0.409990013	0.168819994

The structural file for Mo-IrN$_2$-*NHO

Mo-IrN$_2$-*NHO

1.0

9.5867996216	0.0000000000	0.0000000000
-0.0290030500	11.2661627337	0.0000000000
0.0000000000	0.0000000000	15.0082998276

Ir	N	Mo	O	H
8	19	1	1	1

Direct

0.303680003	0.178849995	0.977630019
0.598389983	0.168860003	0.980069995
0.950230002	0.174349993	0.973309994
0.284040004	0.506280005	0.016729999
0.933369994	0.500230014	0.013080000
0.262149990	0.833989978	0.989799976
0.617950022	0.839550018	0.988799989
0.969269991	0.842899978	0.987569988
0.120360002	0.284520000	0.986630023
0.127079993	0.073380001	0.970830023
0.456539989	0.296620011	0.992749989
0.445069999	0.048799999	0.975690007
0.775089979	0.272610009	0.985580027
0.782239974	0.062050000	0.972519994
0.107940003	0.606260002	0.017279999
0.115759999	0.393959999	0.005150000
0.450379997	0.619750023	0.014280000
0.457390010	0.405039996	0.007660000
0.787129998	0.629040003	0.010170000
0.779280007	0.382360011	0.999310017
0.121979997	0.963410020	0.976459980
0.111350000	0.715929985	0.005720000
0.439680010	0.938730001	0.979300022
0.448309988	0.730260015	0.001340000
0.786520004	0.950269997	0.977140009
0.791289985	0.740379989	0.999440014
0.600920022	0.519829988	0.169729993
0.640950024	0.508029997	0.046700001
0.661239982	0.414440006	0.176090002
0.554480016	0.555469990	0.225400001

The structural file for Ru-IrN_2-*NO_2

Ru-IrN_2-*NO_2

1.0

9.5867996216	0.0000000000	0.0000000000
-0.0290030500	11.2661627337	0.0000000000
0.0000000000	0.0000000000	15.0082998276

Ir	N	Ru	O
8	19	1	2

Direct

0.305099994	0.162359998	0.996779978
0.595950007	0.175339997	0.997950017
0.950169981	0.169269994	0.996510029
0.261070013	0.508539975	0.996959984
0.973089993	0.497330010	0.996999979
0.284069985	0.836499989	0.996290028
0.638170004	0.830429971	0.997590005
0.929120004	0.843500018	0.996429980
0.128629997	0.266930014	0.996749997
0.119159997	0.058610000	0.997080028
0.443459988	0.294569999	0.997340024
0.456860006	0.044539999	0.997669995
0.782859981	0.281349987	0.996749997
0.771690011	0.071709998	0.997470021
0.111270003	0.628740013	0.996569991
0.122850001	0.377119988	0.996810019
0.444150001	0.613479972	0.997039974
0.434689999	0.403759986	0.997120023
0.799589992	0.602150023	0.997070014
0.789979994	0.392250001	0.997290015
0.115130000	0.947250009	0.996919990
0.105499998	0.738940001	0.996309996
0.462449998	0.934099972	0.997250021
0.451310009	0.724399984	0.996339977
0.777270019	0.961269975	0.997569978
0.790730000	0.711329997	0.997030020
0.617120028	0.502969980	0.135800004
0.617169976	0.502950013	0.003110000
0.626630008	0.600350022	0.173030004
0.607620001	0.405699998	0.173160002

The structural file for Ru-IrN$_2$-*NO$_2$H

Ru-IrN$_2$-*NO$_2$H

1.0

9.5867996216	0.0000000000	0.0000000000
-0.0290030500	11.2661627337	0.0000000000
0.0000000000	0.0000000000	15.0082998276

Ir	N	Ru	O	H
8	19	1	2	1

Direct

0.303649992	0.167909995	0.982219994
0.595120013	0.180529997	0.984220028
0.949190021	0.174449995	0.980270028
0.260270000	0.512960017	0.007410000
0.971740007	0.502170026	0.006440000
0.282469988	0.841250002	0.995180011
0.636990011	0.835349977	0.996930003
0.928279996	0.847580016	0.994780004
0.126859993	0.272260010	0.987079978
0.117650002	0.063230000	0.980199993
0.442400008	0.299239993	0.992200017
0.455229998	0.049440000	0.981209993
0.782530010	0.285800010	0.988950014
0.771300018	0.075769998	0.978860021
0.110330001	0.633769989	0.009660000
0.121660002	0.381929994	0.996630013
0.442970008	0.619650006	0.011390000
0.432900012	0.407750010	0.002500000
0.797749996	0.607739985	0.013820000
0.790870011	0.395909995	0.999599993
0.114340000	0.951990008	0.986310005
0.105020002	0.744000018	0.005220000
0.460810006	0.939220011	0.985960007
0.450489998	0.730520010	0.005050000
0.776709974	0.965690017	0.984600008
0.789240003	0.717010021	0.007920000
0.615849972	0.488900006	0.141560003
0.616840005	0.507629991	0.015850000
0.657830000	0.591040015	0.190630004
0.584590018	0.403039992	0.185959995
0.650749981	0.563369989	0.252829999

The structural file for Mo-IrN$_2$-*H

Mo-IrN$_2$-*H

1.0

9.5867996216	0.0000000000	0.0000000000
-0.0290030500	11.2661627337	0.0000000000
0.0000000000	0.0000000000	15.0082998276

Ir	N	Mo	H
8	18	1	1

Direct

0.285420001	0.174930006	0.976149976
0.616559982	0.165279999	0.970380008
0.946720004	0.175090000	0.976310015
0.299039990	0.500150025	0.024480000
0.933759987	0.500349998	0.024390001
0.262340009	0.834699988	0.982050002
0.616100013	0.838479996	0.980409980
0.970009983	0.834290028	0.982230008
0.116219997	0.285620004	0.992079973
0.115759999	0.068640001	0.969560027
0.456039995	0.277590007	0.985390007
0.444669992	0.055590000	0.969280005
0.776669979	0.278160006	0.985650003
0.787850022	0.055280000	0.969349980
0.116540000	0.602919996	0.024289999
0.116319999	0.393579990	0.014780000
0.450639993	0.621439993	0.006210000
0.460370004	0.386350006	0.006240000
0.781710029	0.620970011	0.005750000
0.772119999	0.386889994	0.006330000
0.116070002	0.958480000	0.972190022
0.116329998	0.709890008	0.003700000
0.441570014	0.943539977	0.972159982
0.445980012	0.731260002	0.991760015
0.791010022	0.943310022	0.972140014
0.785979986	0.730920017	0.991680026
0.615509987	0.503329992	0.044300001
0.615130007	0.489450008	0.156680003

The structural file for Ru-IrN_2-*H

Ru-IrN_2-*H

1.0

9.5867996216	0.0000000000	0.0000000000
-0.0290030500	11.2661627337	0.0000000000
0.0000000000	0.0000000000	15.0082998276

Ir	N	Ru	H
8	18	1	1

Direct

0.304140002	0.163010001	0.988820016
0.595200002	0.175329998	0.988680005
0.949760020	0.170340002	0.988009989
0.261059999	0.508780003	0.007230000
0.971419990	0.497590005	0.007220000
0.282730013	0.836030006	0.989160001
0.637300014	0.830969989	0.989629984
0.928349972	0.843309999	0.989690006
0.127890006	0.267729998	0.996760011
0.118270002	0.058920000	0.983169973
0.443250000	0.294059992	0.999499977
0.455520004	0.044650000	0.981890023
0.781250000	0.281230003	0.996179998
0.771399975	0.072080001	0.981760025
0.110519998	0.628830016	0.005410000
0.121979997	0.377510011	0.004330000
0.445780009	0.613969982	0.005030000
0.435900003	0.403470010	0.005670000
0.796649992	0.602900028	0.006900000
0.786670029	0.392379999	0.003970000
0.114160001	0.947380006	0.983569980
0.104610004	0.738669991	0.998210013
0.461100012	0.934170008	0.982240021
0.451229990	0.725160003	0.997550011
0.777000010	0.961589992	0.982190013
0.789279997	0.712339997	0.000920000
0.616310000	0.503170013	0.007970000
0.616060019	0.500410020	0.112149999

Reference

1 J. Jia, S. Wei, Q. Cai and J. Zhao, Two-dimensional IrN_2 monolayer: An efficient bifunctional electrocatalyst for oxygen reduction and oxygen evolution reactions, *J. Colloid Interface Sci.*, 2021, **600**, 711–718.

2 X. Guo, J. Gu, S. Lin, S. Zhang, Z. Chen and S. Huang, Tackling the activity and selectivity challenges of electrocatalysts toward the nitrogen reduction reaction via atomically dispersed biatom catalysts, *J. Am. Chem. Soc.*, 2020, **142**, 5709–5721.